Research Open

Geology, Earth and Marine Sciences
Volume 8 Issue 2

Research Article

Precede High-pressure, High-Temperature Mineralization in the Variscan Tin Deposit Ehrenfriedersdorf/Germany

Rainer Thomas*

Im Waldwinkel 8, D.14662 Friesack, Germany

***Corresponding author:** Rainer Thomas, Im Waldwinkel 8, D-14662 Friesack, Germany

Received: March 16, 2026; **Accepted:** March 20, 2026; **Published:** March 22, 2026

Abstract

This study documents the occurrence of diamond like carbon (DLC) and coesite remnants within pegmatite quartz from the Variscan tin deposit at Ehrenfriedersdorf, Germany. Raman spectroscopic and microscopic analyses reveal both isolated DLC aggregates and a centimetre-scale carbon–quartz network within the root zone of quartz crystals. Quartz within this network preserves spectral features indicative of former coesite, while associated carbon phases show broadened Raman bands characteristic of lonsdaleite-like and metastable diamond-like carbon formed under high-pressure, high-temperature conditions. The textures and mineral associations suggest rapid quenching and a primary origin, rather than secondary contamination. Transport by deep-sourced supercritical fluids is proposed as a mechanism for introducing ultrahigh-pressure material into the evolving pegmatite system, providing new evidence for transcrustal transport during Variscan magmatic and ore-forming processes.

Keywords: *Diamond like carbon (DLC), Lonsdaleite like carbon, Coesite remnants, High pressure–high temperature (HP-HT) mineralization, Pegmatite quartz, Variscan tin deposit, Raman spectroscopy, Supercritical fluids, Ultrahigh pressure minerals, Trans crustal transport*

Introduction

Recent studies have documented the occurrence of ultrahigh-pressure (UHP) mineral phases within crustal granitoids and associated ore systems, challenging conventional models of purely crustal magmatic evolution (see the discussion by Schütze et al., 1983 [1], which first suggested the involvement of components derived from depths of up to ~115 km, corresponding to pressures of ~60 GPa). In particular, the identification of diamond, diamond-like carbon (DLC), and related high-pressure carbon phases in the Variscan tin deposit of Ehrenfriedersdorf (Germany) has provided compelling evidence for a transient interaction between shallow magmatic systems and deep-seated, high-pressure environments [2,3]. These observations imply the operation of previously underappreciated transport mechanisms capable of transferring UHP material across large crustal depth intervals within geologically short timescales. Building on earlier reports of moissanite–diamond–graphite parageneses and isolated DLC inclusions in quartz and accessory minerals from Ehrenfriedersdorf, continued investigation of archival sample material has revealed additional, more systematic evidence for high-pressure carbon phases [4]. Most previously described DLC occurrences consist of small, isolated aggregates randomly distributed within low-quartz, topaz, fluorite, cassiterite, or beryl. In these host minerals, the presence of such phases is highly unexpected under normal crustal pressure–temperature conditions, raising fundamental questions concerning their origin, timing, and mode of incorporation. These observations extend beyond interpretations involving shock-related nanodiamond formation or whisker growth (e.g., moissanite or diamond) via natural chemical vapor deposition (CVD) processes driven by reduced CH_4–H_2–H_2O–CO_2 supercritical fluids [4]. During renewed, particularly careful microscopic screening of pegmatite quartz from the well-studied sample Qu8, special attention was paid to crystal root zones, which are commonly neglected due to their high inclusion density and analytical complexity. This approach led to the discovery of a centimetre-scale carbon–quartz assemblage forming an irregular, network-like structure within the root zone of a quartz crystal. Unlike previously reported isolated DLC grains, this network contains abundant carbon phases spatially associated with quartz that preserves Raman spectroscopic signatures indicative of former coesite. The coexistence of coesite remnants with lonsdaleite-like and diamond-like carbon implies formation under high-pressure, high-temperature (HP–HT) conditions, followed by rapid quenching. The present contribution documents the textural relationships, Raman spectroscopic characteristics, and mineralogical context of this carbon–quartz network. By contrasting these features with those of isolated DLC occurrences, this study aims to demonstrate that high-pressure carbon phases in the Ehrenfriedersdorf pegmatite system are not merely sporadic contaminants but may represent a primary feature of an early evolutionary stage of pegmatite formation. Transport by deep-sourced supercritical fluids is discussed as a plausible mechanism for introducing UHP material into the developing pegmatite system, providing further evidence for transcrustal transport processes operating during Variscan magmatic and ore-forming events.

Sample and Methods

Sample Description

The pegmatite quartz sample most frequently investigated in this study, designated **Qu8**, has been described in detail by Thomas et al. (1998) [5] and Thomas and Webster (2000) [6]. The sample originates from a large, granular-to-disc-shaped pegmatite body measuring approximately $2 \times 10 \times 10$ m, exposed in the granite endocontact at the fifth gallery near the main shaft of the Sauberg mine, Ehrenfriedersdorf, Germany. The material was collected in 1987. The studied quartz crystals are mostly water-clear and exhibit well-developed prismatic morphologies and internal growth zoning. The host pegmatite contains a diverse mineral assemblage, including orthoclase (locally enriched in P_2O_5 up to 1.3 wt%), albite, beryl, topaz, cassiterite, fluorite, and numerous phosphate minerals such as apatite, amblygonite, berlinite, and isocite. Previous investigations of sample Qu8 primarily employed electron microprobe techniques with deposited carbon coatings. As a consequence, indigenous carbon phases—particularly diamond-like carbon (DLC)—were commonly overlooked. In addition, the root zones of quartz crystals were rarely examined because of their high inclusion density and analytical complexity. These zones, however, are shown here to be critical for recognizing high-pressure carbon–silica assemblages.

Analytical Methods

The analytical approach applied in this study follows established methodologies previously described in detail by Thomas et al. (1998) [5], Rickers et al. (2006) [7], Thomas and Davidson (2012) [8], and Borisova et al. (2012) [9]. Sample Qu8, with its exceptionally high abundance of melt, fluid, and mineral inclusions, has long served as a reference material for the development and application of microanalytical techniques. In the present contribution, emphasis is placed on **optical microscopy** and **Raman spectroscopy**, which together serve as essential preliminary tools for identifying diamond-like carbon, lonsdaleite-like carbon, and coesite remnants prior to further analytical work.

Optical Microscopy

Petrographic investigations were carried out using a **Zeiss JENALAB POL** polarization microscope in both transmitted and reflected light modes. This instrument was used to identify diamond-like crystals hosted in quartz, associated paragenetic minerals, and characteristic textural relationships.

Selected areas were subsequently examined using an **Olympus BX43** microscope coupled to a Raman spectrometer. The system is equipped for both transmitted and reflected polarized-light microscopy and includes rotating and X–Y stages, allowing precise positioning and orientation of inclusions and microstructures within the quartz crystals.

Raman Spectroscopy

Raman spectroscopy was performed to identify carbon phases and silica polymorphs. Between 1992 and 2020, several Raman systems were employed (Raman Probe MRL1000; Dilor XY Laser Raman Triple 800 mm; LabRAM UV HR 800), using excitation wavelengths of 633, 514, 488, and 325 nm. The data presented here were acquired using an **EnSpectr Raman microscope (RamMics R532)**.

Measurements covered the spectral range from 0 to 4000 cm^{-1} and were conducted with a single-mode 532 nm laser operating at a maximum output of 50 mW. Analytical settings included a 20 µm entrance aperture, a holographic grating of 1800 g mm^{-1}, and a spectral resolution of approximately 4 cm^{-1}. For most analyses of diamond-like carbon, a long-working-distance **Olympus LMPlanFL 100×** objective was used. Laser power at the sample surface was continuously adjustable down to 0.02 mW. Because elevated laser energies can induce partial or complete transformation of microdiamonds into carbon, analytical measurements were performed at laser powers ≤ 5 mW. Higher powers (up to 30 mW) were applied only for overview scans and sample mapping.

Raman band positions were calibrated before and after each measurement series using the Si band of a semiconductor-grade single-crystal silicon chip. Based on 20 repeated measurements, run-to-run reproducibility was ± 0.3 cm^{-1} for silicon (520.4 ± 0.3 cm^{-1}) and ± 0.5 cm^{-1} for diamond (1332.3 ± 0.5 cm^{-1}) over the spectral range from 50 to 2000 cm^{-1}. The full width at half maximum (FWHM) of the diamond reference peak was 4.8 ± 0.1 cm^{-1}. A water-clear natural diamond crystal from Brazil served as an external reference standard. An additional advantage of the Raman system used is its reliable, straightforward zero-point calibration.

Methodological Focus

The combined use of high-resolution optical microscopy and carefully controlled Raman spectroscopy proved essential for identifying rare, optically camouflaged high-pressure phases within inclusion-rich pegmatite quartz. Particular attention was paid to quartz root zones, which are commonly excluded from routine studies but are shown here to preserve critical evidence for high-pressure–high-temperature processes.

Key Observations

The pegmatite quartz contains many fluid and melt inclusions and, for a pegmatite, typical mineral inclusions. Table 1 presents a selection of daughter mineral phases, mostly found in pegmatite quartz.

One part of the shown daughter mineral phases also appears as solid mineral inclusions in quartz. Rare examples include berlinite and boric acid (sassolite); the latter was found between cassiterite crystals in sample Sn70 [10]. The great variety of inclusions and minerals in the quartz sample masks the presence of small and rare DLCs. Figures 1 and 2 show two typical fluid inclusions in the pegmatite quartz Qu8, of this size and frequency, ideal for camouflaging unusual inclusions.

Figure 2 shows another fluid inclusion type with a relatively large sphalerite daughter crystal beside muscovite in a NaCl-KCl-H_3BO_3-rich solution. This sphalerite daughter crystal is nearly water-clear, similar to the sphalerite in beryl [3]. Ore-forming sphalerite is present in the deposit; however, mostly jet-black, as the so-called christophite.

Table 1: Some typical daughter mineral phases in fluid and melt inclusions in granite and pegmatite minerals from the Variscan Erzgebirge, mostly determined with Raman spectroscopy (mainly after Thomas and Davidson, 2012) [8]. Inclusion type: F = fluid inclusion, M = melt inclusion. Localities: 1 = Ehrenfriedersdorf (Sauberg, Greifenstein), 2 = Eibenstocker granite, 3 = Podlesi granite, 4 = Zinnwald, Altenberg. (Rb,Cs,K)-Zn-tetrachloride is a new mineral phase in fluid inclusions in the pegmatite quartz from Ehrenfriedersdorf, identified using Raman spectroscopy, SYRFA, and Laser ICP microanalysis; however not proposed to the IMA – it is a variety of the mineral flinteite [$K_2(ZnCl)_4$].

Mineral	Formula	Locality	Inclusion type
Graphite	C	1	F, M
Diamond	C	1	F
Sulfur	S	4	F
Arsenic	As	1	F
Arsenolite	As_2O_3	3	F
Sassolite	H_3BO_3	1,2,3,4	F, M
Metaboric acid I	HBO_2	1	F
Cristobalite	SiO_2	1	F
Cristobalite-X-I	SiO_2	1	F
Coesite	SiO_2	1	F
Cassiterite	SnO_2	1,2,3,4	F, M
Orthorhombic cassiterite	o-SnO_2	1,2,4	F, M
Hematite	Fe_2O_3	1,2,4	F
Sphalerite	ZnS	1	F
Bromargyrite Br: Cl~1: 1)	Ag(Br,Cl)	1	F
Halite	NaCl	1,2,3,4	F
Sylvite	KCl	1,2,3,4	F
Cryolite	Na_3AlF_6	1,2,4	F
Elpasolite	K_2NaAlF_6	1,4	F
Cryolithionite	$Na_3Li_3Al_2F_{12}$	1,2,4	F
Hieratite	K_2SiF_6	4	F
Avogadrite	$(K,Cs)BF_4$	1,2,4	F
Rb-Flinteite	$(K,Rb,Cs)_2ZnCl_4$	1	F
SnF_2 (no mineral name)	SnF_2	4	F
Nahcolite	$NaHCO_3$	1,2,3,4	F, M
Zabuyelite	Li_2CO_3	1,2,4	F, M
Dawsonite	$NaAl(CO_3)(OH)_2$	1	F, M
Ramanite-(Cs)	$Cs_2B_3O_8 \cdot 4H_2O$	1,2	F, M
Beryllonite	$NaBePO_4$	1	F
Hambergite	$Be_2BO_3(OH,F)$	1	F, M
OH-Herderite	$CaBePO_4(F,OH)$	1	F
Berlinite	$AlPO_4$	1	M
Muscovite	$KAl_4Si_5Al_2O_{20}(OH,F)_4$	1,2,3,4	F, M

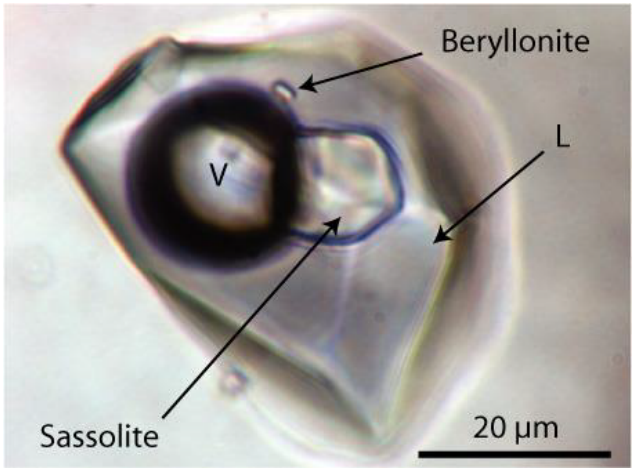

Figure 1: Fluid inclusion in pegmatite quartz (Qu8) from the Sauberg mine near Ehrenfriedersdorf/Germany. Daughter minerals are beryllonite [$NaBePO_4$], and sassoline [H_3BO_3], L - solution, V - vapor.

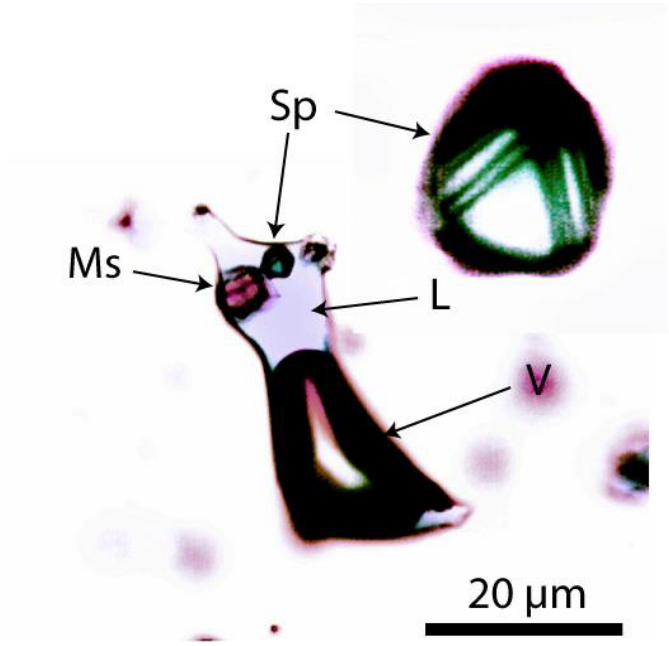

Figure 2: Vapor-rich fluid inclusion in pegmatite quartz, Qu8, with a Fe-poor nearby colorless sphalerite crystal (Sp). An enlargement of this crystal is right at the top. L – NaCl-KCl-H_3BO_3-rich solution, Ms – muscovite, V – CO_2-CH_4-rich vapor phase.

Table 2: High-pressure quenched lonsdaleite/diamond-like carbon in the foreign quartz-carbon aggregate (Figure 3) in pegmatite quartz (see also Table 1 in Thomas, 2026) [4].

Lonsdaleite-like carbon (cm^{-1})	FWHM (cm^{-1})	G-band (cm^{-1})	FWHM (cm^{-1})	n
1326.8 ± 1.7	54.6 ± 18.8	1570.4 ± 2.6	71.8 ± 8.0	12
1324.5 ±1.6	21.4 ± 4.2	-	-	14

n – number of measured points. Laser power on sample: 4.3 mW.

Such inclusions demonstrate the importance of daughter mineral phases for the estimation of the composition of ore-forming fluids. However, they mask rare and distinct minerals we normally do not encounter. Such a small aggregate is the leaf-like carbon with a whisker-like stalk [4]. Another type is an isolated quartz-carbon aggregate shown in Figure 3a. The quartz of this inclusion is very different to his low-quartz host – fine-grained and surrounded by a thin carbon film. The quartz contains indications of coesite (Figure 3b).

Figure 3b shows the remnant of the primary present coesite band at 517.5 cm^{-1}. Other lines are also present; however, in most cases, they are weak: 74.5 (vs), 202 (w), 355 (w), 784.7 ± 2.6 (m) – all in cm^{-1} [11]. The letters in brackets mean the Raman intensity: vs – very strong, m – medium, w – weak.

The carbon part of the inclusion (Figure 3a) contains many micrometer-large lonsdaleite-like carbon crystals (Table 2).

The lonsdaleite-like carbon in the second row shows practically no G-band (only a background). At least the observation of more or less isolated DLC aggregates "swimming" in the pegmatite quartz is, up to now, the state of knowledge. By careful screening of the root zone of a quartz crystal from the sample collective Qu8, we found a remarkable "network" of carbon (Figure 4) and formerly coesite (now only visible by Raman, with some typical coesite bands).

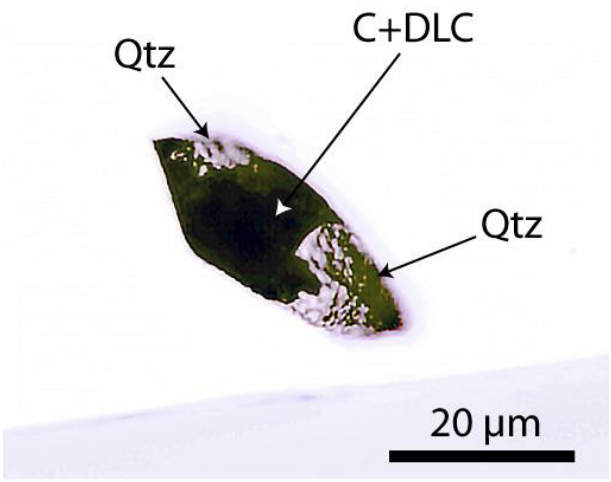

Figure 3a: Isolated foreign aggregate of carbon and quartz (Qtz) - formerly coesite - in transparent pegmatite low-quartz Qu8 from Ehrenfriedersdorf.

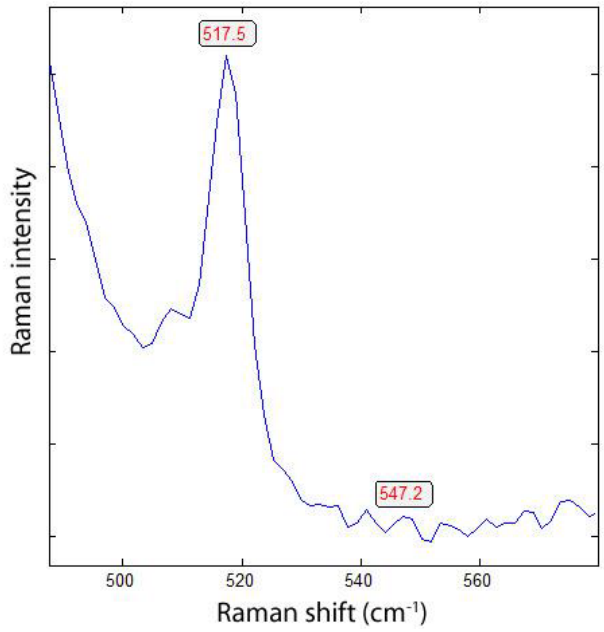

Figure 3b: Main band of coesite of the quartz part of the inclusion in Figure 3a.

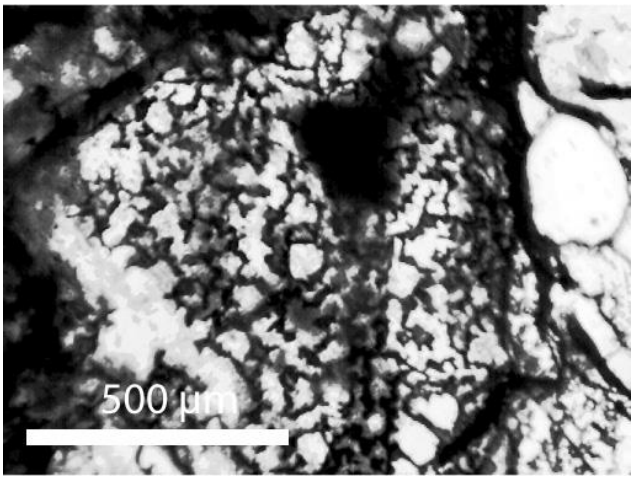

Figure 4a: Carbon-quartz network with coesite remnants in between in the root zone of the pegmatite quartz Qu8.

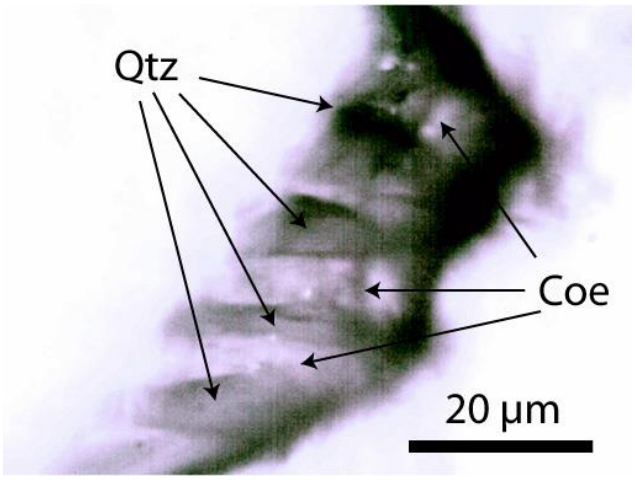

Figure 4b: Quartz (Qtz)-coesite (Coe)-carbon lamella in Figure 4a. The black part is carbon-rich.

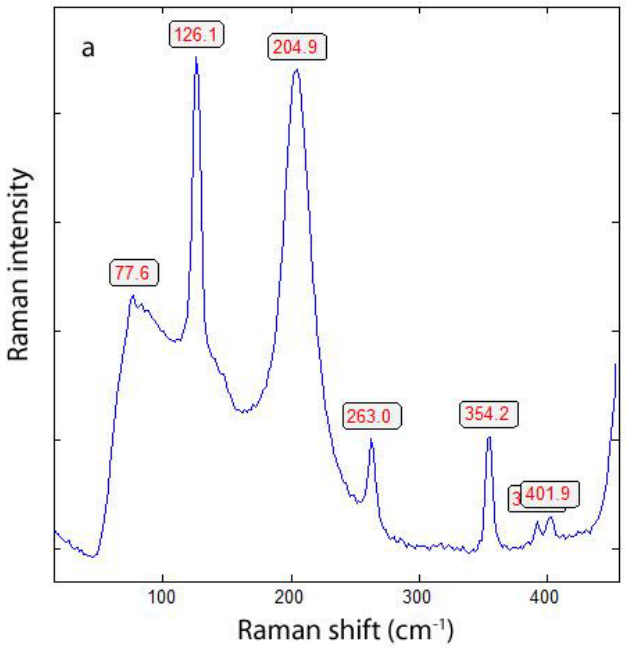

Figure 5a: Raman spectrum of coesite-like quartz in the carbon "network" – low frequency range without the very strong quartz band at 464 cm^{-1}. The band at 77.6 cm^{-1} is often very strong, with an intensity comparable to that of the quartz main band at 464 cm^{-1}.

The quartz shows, as a rule (see Hemley, 1987) [11], an adjacent linear, low-intensity background between 50 and 450 cm^{-1}. Quartz with remnants of coesite, on the other hand, shows, between 50 and 300 cm^{-1}, a strong increase and drop in intensity (see Figure 5a). Somtimes is the intensity of the Raman band at about 75 cm^{-1} equeal or higher than the quartz main band at 464 cm^{-1}.

Using a small Raman window from 490 to 580 cm^{-1} for the measurement of the coesite main line, a value of 516.0 ± 2.3 cm^{-1} (n = 13) is obtained. Figure 6 shows such Raman spectra (Figures 6-9).

Table 3 summarizes the Raman measurements on DLC in the "network" part of the root zone of a quartz crystal; the data around 1323 cm^{-1} corresponds to lonsdaleite-like diamond. The FWHM values are the opposite of those of well-crystallized diamond, generally very large: >25 cm^{-1} vs 4 cm^{-1}.

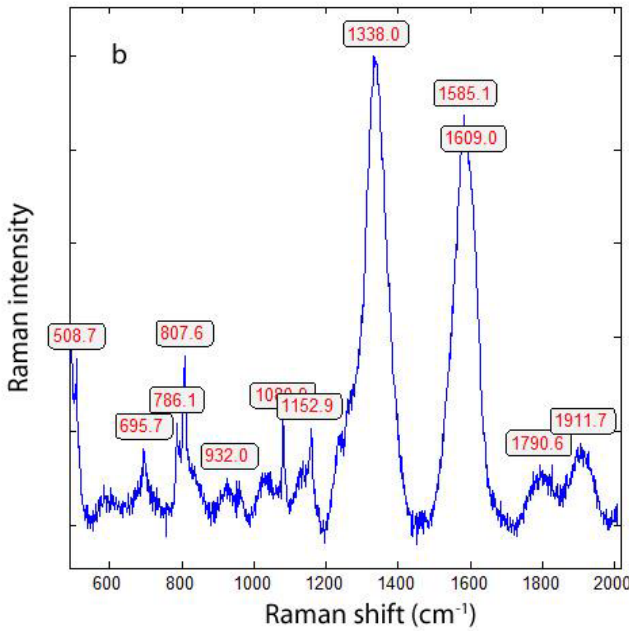

Figure 5b: Raman spectrum of coesite-like quartz and DLC in the "network" – high frequency range without the very strong quartz band at 464 cm^{-1}, taken at 10 mW. The position of the DLC band at 1338 cm^{-1} may result from heating caused by the higher laser power (see Zaitsev, 2001) [12] and the black surroundings.

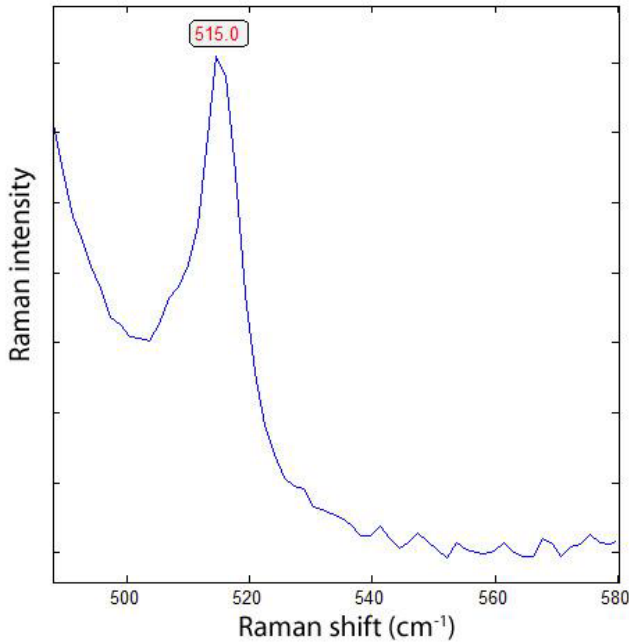

Figure 6: Coesite main band (515 cm^{-1}) in quartz of the " carbon network", similar to Figure 3b.

Table 3: High-pressure quenched DLC in the quartz-carbon "network" (Figure 4) in the root zone of the pegmatite quartz (see also Table 1 in Thomas, 2026). Laser power: 4.3 mW.

DLC (cm^{-1})	FWHM (cm^{-1})	G-band (cm^{-1})	FWHM (cm^{-1})	n
1335.8 ± 2.9	67.2 ± 15.6	1577.5 ± 5.7	71.4 ± 10.1	12
1332.0 ± 2.8	81.8 ± 3.9	1588.3 ± 8.9	77.6 ± 1.0	9
1323.8 ± 2.1	25.6 ± 8.8	1572.3 ± 4.7	67.4 ± 8.8	27
1323.5 ± 0.2	76.7 ± 1.8	1486.9 ± 1.4*	40.8 ± 3.4	9

*According to Zaitzev (2001) [12] that is a quenchable metastable carbon phase consisting of an amorphous mixture of four-fold coordinated diamond and three-fold coordinated graphitic carbon. n – number of measured crystals.

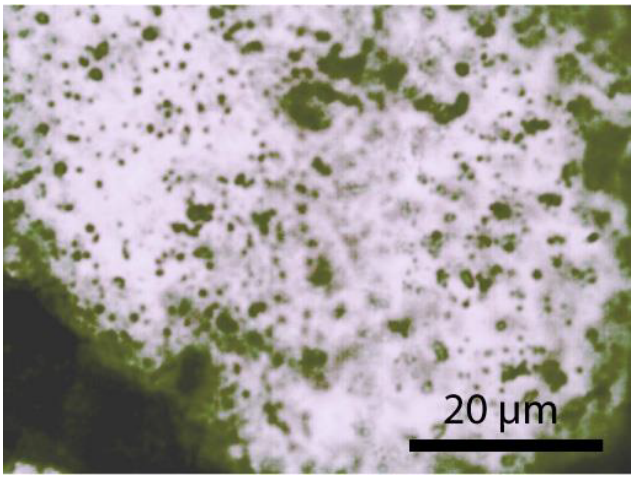

Figure 7: Quartz and coesite remnants inside the carbon "network" containing many small black carbon and DLC crystals.

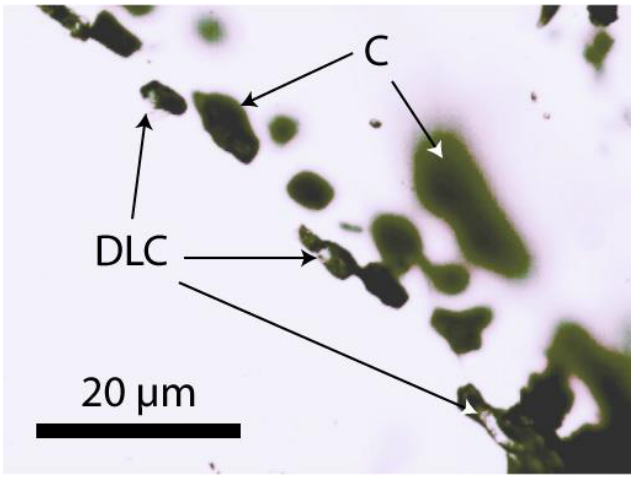

Figure 8: Carbon (C) in pegmatite quartz (Qu8) with small DLC crystallites.

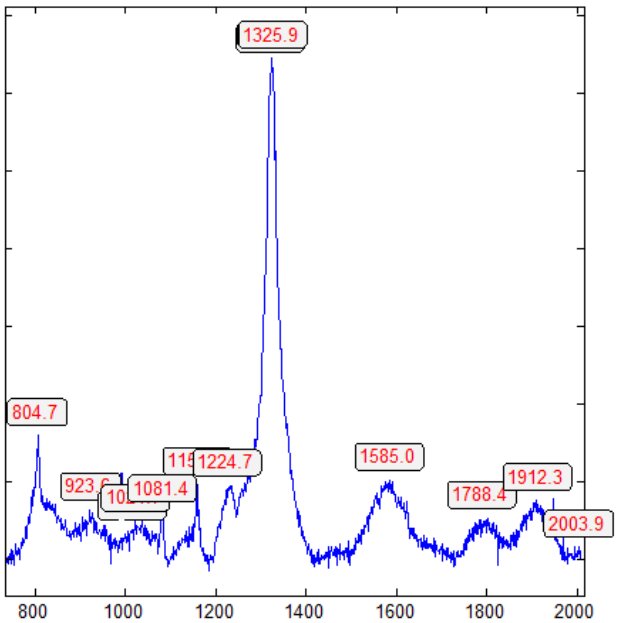

Figure 9: DLC in pegmatite quartz-carbon network (about 65 µm under the sample surface).

Interpretation

Up to now, all found DLC crystals are generally rare, statistical distributed small aggregates. The found carbon-quartz "network" at the root zone of a quartz crystal is irregularly formed and measures about 2 x 0.5 cm. Transport via supercritical fluid (SCF) is conceivable at an early stage in the formation of the pegmatite chamber. Is maybe the embryonic stage of this chamber. Due to the high velocity of the SCF, larger rock fragments from greater depths (at pressures and temperatures of 4 to 6 GPa and 1000 to 1500°C) can also be transported. The SCF can, of course, come from greater depths.

Discussion

The observations presented in this contribution extend earlier reports of ultrahigh-pressure (UHP) mineral phases associated with the Variscan tin mineralization at Ehrenfriedersdorf and provide new textural evidence for their primary incorporation into pegmatite quartz. In contrast to previously described isolated diamond-like carbon (DLC) aggregates, the discovery of a centimetre-scale carbon–quartz "network" in the root zone of a quartz crystal indicates that high-pressure carbon phases were not merely sporadic contaminants but may represent a more systematic feature of an early evolutionary stage of the pegmatite system. Raman spectroscopic data demonstrate that quartz within this network preserves remnants of coesite, as evidenced by characteristic low-frequency bands and a main band near 515–517 cm^{-1}. These spectral features clearly distinguish the network quartz from the surrounding low-quartz host and indicate a former stability field well outside normal crustal conditions. The coexistence of coesite remnants with lonsdaleite-like and diamond-like carbon, characterized by broadened Raman bands and large FWHM values, is consistent with rapid quenching from high-pressure, high-temperature conditions. Such spectral characteristics suggest structurally disordered or metastable carbon phases rather than well-crystallized diamond. Textural relationships further support a primary origin of the carbon–quartz assemblage. The fine-grained quartz enclosed by carbon films and lamellae contrasts sharply with the optically homogeneous pegmatite quartz host, implying mechanical or chemical isolation prior to final crystallization. The network-like geometry, rather than discrete inclusions, argues against late-stage infiltration or secondary carbon precipitation and instead points to syn- or pre-pegmatitic incorporation. Transport by a supercritical fluid (SCF) offers a plausible mechanism for introducing such exotic assemblages into the upper crust. An SCF capable of operating at pressures of several GPa and temperatures exceeding 1000 °C could entrain fragments of deeper material, including coesite-bearing silica and high-pressure carbon phases, and deliver them rapidly into a developing pegmatite chamber. The observed preservation of coesite remnants and metastable carbon phases is consistent with rapid ascent and cooling, limiting complete back-transformation to low-pressure polymorphs. Overall, the data support a model in which the Ehrenfriedersdorf pegmatite system records an early, transient interaction with deep-seated, high-pressure materials. The carbon–quartz network documented here represents a rare snapshot of this process and strengthens the case for transcrustal transport mechanisms operating during Variscan magmatic and ore-forming events. Further systematic screening of quartz root zones may reveal that such features are more common than previously recognized, but commonly overlooked due to their optical camouflage within inclusion-rich pegmatite quartz.

Acknowledgment

The author thanks colleagues and collaborators for longstanding discussions on high-pressure mineral phases and the application of Raman spectroscopy to fluid and mineral inclusions. Access to archival sample material from the Ehrenfriedersdorf pegmatite system, collected during earlier underground work at the Sauberg mine, is gratefully acknowledged. Constructive comments from reviewers and editors, which helped to improve the clarity and focus of this contribution, are also appreciated.

References

1. Schütze H, Stiehl G, Wetzel K, Beuge P, Haberlandt R, et al. (1983) Isotopen- und elementgeochemische sowie radiogeochronologische Untersuchungen an der Zinnlagerstätte Ehrenfriedersdorf. Akademie der Wissenschaften der DDR, Zentralinstitut für Isotopen- und Strahlenforschung Leipzig, Zfl-Mitteilungen, Nr. 76: 232-271.
2. Thomas R, Davidson P, Rericha A, Recknagel U (2023a) Ultrahigh-pressure mineral inclusions in a crustal granite: Evidence for a novel Transcrustal transport mechanism. *Geoscience* 13: 1-13.
3. Thomas R, Recknagel U, Rericha A. (2023b) A moissanite-diamond-graphite paragenesis in a small beryl-quartz vein related to the Variscan tin-mineralization of the Ehrenfriedersdorf deposit, Germany. *Geosciences* 13: 1-13.
4. Thomas R (2026) Finding of lonsdaleite-like carbon in pegmatite quartz from the Sauberg mine near Ehrenfriedersdorf/Germany. *Geology, Earth and Marine Sciences* 8: 1-5.
5. Thomas R, Webster JD, Rhede D (1998) Strong phosphorus enrichment in a pegmatite-forming melt. *Acta Universitatis Carolinae – Geologica* 42: 150-164.
6. Thomas R, Webster JD (2000) Strong tin enrichment in a pegmatite-forming melt. *Mineral Deposita* 35: 570-582.
7. Rickers K, Thomas R, Heinrich W (2006) The behavior of trace elements during the chemical evolution of the H_2O-, B-, and F-rich granite-pegmatite-hydtothermal system at Ehrenfriedersdorf, Germany: a SXRF study of melt and fluid inclusions. *Mineralium Deposita* 41: 229-245.
8. Thomas R, Davidson P (2012) The application of Raman spectroscopy in the study of fluid and melt inclusions. Z. dt. *Ges Geowiss* 163: 113-126.
9. Borisova AY, Thomas R, Salvi S, Candaudap F, Lanzanova A, Chmeleff J (2012) Tin and associated metal and metalloid geochemistry by femtosecond LA-ICP-QMS microanalysis of pegmatite-leucogranite melt and fluid inclusions: new evidence for melt-melt-fluid immiscibility. *Moneralogical Magazine* 76: 91-113.
10. Thomas R (2024) The $CaCl_2$-to-rutile phase transition in SnO_2 from high to low pressure in nature. *Geol Earth Mar Sci* 6: 1-4.
11. Hemley RJ (1987) Pressure dependence of Raman spectra of SiO_2 polymorphs: a-quartz, coesite, and stishovite. In: High-pressure Research in Mineral Physics, eds. By MH Manghnani and Y Syono. Pg: 347-359.
12. Zaitsev AM (2001) Optical properties of diamond. A data handbook. *Springer*. Pg: 502.
13. Thomas R (2002) Determination of the H_3BO_3 concentration in fluid and melt inclusions in granite pegmatites by laser Raman microprobe spectroscopy. *American Mineralogist* 87: 56-68.
14. Thomas R, Baumann L (1980) Ergebnisse von thermometrischen und kryometrischen Untersuchungen an Kassiteriten des Erzgebirges. Zeitschrift für geologische Wissenschaften. 8(10): 1281-1299.
15. Thomas R (2000) Determination of water contents of granite melt inclusions by confocal laser Raman microprobe spectroscopy. *American Mineralogist* 85: 868-872.

Citation:

Thomas R (2026) Precede High-pressure, High-Temperature Mineralization in the Variscan Tin Deposit Ehrenfriedersdorf/Germany. *Geol Earth Mar Sci* Volume 8(2): 1-6.